Energy 163 (2018) 766–781

Contents lists available at ScienceDirect

Energy

journal homepage: www.elsevier.com/locate/energy

Temporally explicit and spatially resolved global offshore wind energy potentials

Jonathan Bosch [a, b, *], Iain Staffell [c], Adam D. Hawkes [b]

[a] Grantham Institute, Climate Change and the Environment, London, SW7 2AZ, UK
[b] Department of Chemical Engineering, Imperial College London, London, SW7 2AZ, UK
[c] Centre for Environmental Policy, Imperial College London, London, SW7 1NE, UK

ARTICLE INFO

Article history:
Received 2 July 2018
Received in revised form
3 August 2018
Accepted 20 August 2018
Available online 23 August 2018

Keywords:
Offshore wind energy
Wind energy potentials
GIS
Intermittency
Energy systems models
Renewables modelling

ABSTRACT

Several influential energy systems models (ESMs) indicate that renewable energy must supply a large share of the world's electricity to limit global temperature increases to 1.5 °C. To better represent the costs and other implications of such a transition, it is important that ESMs can realistically characterise the technical and economic potential of renewable energy resources. This paper presents a Geospatial Information System methodology for estimating the global offshore wind energy potential, i.e. the terawatt hour per year (TWh/yr) production potential of wind farms, assuming capacity could be built across the viable offshore area of each country. A bottom-up approach characterises the capacity factors of offshore wind farms by estimating the available wind power from high resolution global wind speed data sets. Temporal phenomena are retained by binning hourly wind speeds into 32 time slices per year considering the wind resource across several decades. For 157 countries with a viable offshore wind potential, electricity generation potential is produced in tranches according to the distance to grid connection, water depth and average annual capacity factor. These data can be used as inputs to ESMs and to assess the economically viable offshore wind energy potential, on a global or per-country basis.

1. Introduction

Since the Intergovernmental Panel on Climate Change's (IPCC) 5th Assessment report (AR5) [1], world governments have come to a consensus that global average temperatures should not exceed 2 °C above pre-industrial levels to avoid dangerous climate change this century. The Paris agreement (COP21) [2] also included a non-binding commitment to "pursue efforts" in limiting the temperature increase even further to 1.5 °C, recognising new scientific understanding on the ecological and societal impacts of this level of warming [3].

It is estimated that cumulative carbon (equivalent) emissions between 2000 and 2050 must stay below 1440 gigatons of carbon dioxide (Gt CO_2) to assure a 50% probability of limiting temperature increases to 2 °C [4,5]. These required CO_2 reductions are concurrent with a predicted increase in global energy demand [6]. The World Energy Council (WEC) and the International Energy Agency (IEA) see total primary energy consumption increasing from 563 EJ in 2015 to between 663 and 879 EJ in 2050 (a 17–56% increase) [7–9].

Most mitigation scenarios produced by Integrated Assessment Models (IAMs) suggest significant deployment of VRE technologies is needed up to 2050 because of their potential to decarbonise the electricity sector [1,9,10]. Many IAMs can only produce viable future global energy systems by drawing on renewable, and even negative emissions, technologies to reach its prescribed climate target [1]. The IPCC's 5th Assessment Report scenario database (2014) employed 31 models producing 1184 scenarios, many of which have been criticised for their over-reliance on negative emissions technologies [11,12].

However, without reasonable bounds on the potential of wind energy, energy systems models (ESMs) with insufficient detail in renewable resource characteristics and VRE technologies could mislead researchers and policy makers into believing the potential for large scale deployment is much greater than it really is. Indeed, much work in the literature suggests that a 100% renewable energy system could be achieved through expected technological advancements and cost reductions [12–14]. However, recent research

* Corresponding author. Grantham Institute, Climate Change and the Environment, London, SW7 2AZ, UK.
E-mail address: j.bosch14@imperial.ac.uk (J. Bosch).

https://doi.org/10.1016/j.energy.2018.08.153

Nomenclature

AEP	Annual energy production
AR5	Fifth assessment report of the IPCC
CAPEX	Capital expenditure
DTU	Technical University of Denmark
EEZ	Exclusive economic zone
EJ	Exajoule (10^{18} J)
ESM	Energy system model
EU	European Union
GIS	Geographic information system
GW	Gigawatts
GWA	Global wind atlas
GWh	Gigawatt-hours
IAM	Integrated assessment model
IEA	International Energy Agency
IPCC	Intergovernmental Panel on Climate Change
LCOE	Levelised cost of electricity
MERRA-2	Modern-Era Retrospective analysis for Research and Applications, Version 2
MW	Megawatts
MWh	Megawatt-hours
NASA	National Aeronautics and Space Administration
NREL	National Renewable Energy Laboratory (US)
O&M	Operations and maintenance
OPEX	Operating expenditure
OWE	Offshore wind energy
TWh/yr	Terawatt-hours per year
VRE	Variable renewable energy
WEC	World Energy Council

suggests geographical and efficiency constraints imposed in many studies on the wind resource have been insufficient, and that wind energy potentials are generally overstated [15,16].

Estimates of the global wind energy potential vary by a wide range (Table 1). This range of estimates can result in a wide range of future scenarios about the extent that renewable technologies can contribute to mitigation. High values of capacity density in those studies leads to large predictions of generation potential, even though efficiency reductions due to the close proximity of turbines does not allow wind farms to reach their estimated power output. Furthermore, early studies using geographic information systems (GIS) methodologies (Archer [17]; Lu [18]) used scarce and low resolution wind speed data, meaning that at the country or global scale, much wind power at the mesoscale – and in locations that are favourable for wind farm deployment – are overlooked. Other approaches, such as Miller's [19] top down estimation, yield some of the lowest estimates because they assume only a certain portion of the kinetic energy from the atmospheric boundary layer can be converted to electrical energy by turbines, without modelling the power conversion explicitly.

In this paper, a Geographical Information Systems (GIS) methodology is used to generate estimates for the bounds of global offshore wind energy potentials, considering several critical parameters which are important underpinning for policy and investment planning. High resolution capacity factors (CF) are developed using a novel calibration of two wind speed data sources, retaining their temporal characteristics, and averaged from several decades of reanalysis data. The exploitable resource is constrained by water depth and surface area suitability, while the terawatt-hour (TWh) generation potential is presented per country and with respect to the distance from the coast and water depth. Energy systems modellers can use these data to consider proximity to population centres and capital costs in their analyses. Furthermore, temporal and spatial specificity are retained in the results, improving the ability to assess intermittent supply of renewable energy.

2. Background

Many areas of energy research have been interested in estimates of the global offshore wind energy potential. IAMs are most concerned with setting boundaries for economic wind energy exploitation by current and future technologies. The temporal (intermittency) and spatial (geographical) characteristics of the wind resource make it difficult for many IAMs to accurately represent the capacity potential of wind energy technologies. Estimates of the capacity potential need to account for a range of constraints and parameters, such as spatial proximity to the grid, water depth, and other considerations that impact investment and operational costs.

2.1. Offshore wind as a viable mitigation technology

In 2017 the biggest capacity additions were VRE despite historic low oil prices (2015–17). Wind continues to be the lowest cost and highest growth area with 539 GW (GW) of additions [24]. This trend is expected to continue with investments in solar and wind, making up 73% of investment in power generation capacity from 2017 to 40 [25]. Offshore wind is an important renewable resource because it competes less with other land uses and has faced less public opposition, while producing a more reliable (less intermittent) energy supply than onshore wind. Offshore farms can additionally reach

Table 1
Literature estimates of wind energy potentials.

Estimated energy potential (EJ/year)	Spatial scope	Constraint	Capacity density (MW/km^2)	Authors
2112	Global onshore	CF $\geq$ 15%	6.25	Bosch et al. [20]
709	Global on/offshore	$EROI_{min}$[a] = 5	2–9	Dupont et al. [15]
3024	Global on/offshore	CF $\geq$ 20%	9/5.85	Lu et al. [18]
153	Europe on/offshore	$V_{10m} \geq 4$ m/s	10/6.4	EEA [21]
2256	Global on/offshore	$V_{80m} \geq 6.9$ m/s	9/9	Archer and Jacobson [17]
2720	Global on/offshore	CF $\geq$ 18%	5/5	Eurek et al. [22]
250–1200	Global on/offshore	$V_{80m} \geq 6.9$ m/s	N/A	GEA [23]
570–2150	Global on/offshore	Top-down	N/A	Miller et al. [19]

CF = Capacity Factor
V_{xxm} = wind velocity at "xx" metres above ground.
[a] Energy Returned on Energy Invested – a minimum constraint.

higher power densities with taller and larger turbines with fewer constraints on size and noise pollution [26]. Offshore wind turbines have grown in nameplate capacity in recent years, and industry experience is allowing them to be developed in deeper waters and further offshore [27]. This trend, along with a fall in the cost of capital [28] has caused offshore wind economics to improve rapidly in recent years.

In 2017, Final Investment Decisions (FID) for UK offshore projects were reaching a levelised cost of energy (LCOE) below £100/MWh (€112/MWh), four years earlier than expected [29]. Projects reached a weighted average strike price of £62.14 (LCOE of £55/MWh) for projects commencing in 2021/22, compared to £142/MWh (€163/MWh) in 2010/11. Danish and Dutch wind farms have yielded lower prices compared to the UK, with awarded strike prices of €61.75/MWh and €72.70/MWh, respectively [30].

Furthermore, although the offshore wind market has so far been dominated by countries with shallow water depths, falling costs and intensifying decarbonisation imperatives have caused many countries to consider the potential of floating offshore wind installations. Research on floating structures for wind turbines is starting to deliver full scale prototypes, but these are still in the early production stages (Hywind project, by Statoil, began production in October 2017). Floating wind also offers cost benefits in the decommissioning stage, although these costs are only a small proportion of total capital expenditures (CAPEX) [31]. Furthermore, leading concepts already expect costs of £85–95/MWh (€97–108/MWh), with further reductions over time because of industrialised production routes [31].

2.2. Integrated assessment modelling of wind energy

To better assess the viability of energy systems with large shares of VRE, ESMs must be able to interpret highly resolved temporal and spatial input data to simulate energy supply characteristics.

However, global IAMs used for projecting future emissions reductions only represent the energy system in an aggregated fashion because they focus on long-term trends between global regions where there is inherently a great deal of uncertainty [32,33]. In contrast to conventional energy sources that can be modelled with known or inferred limits to resource supply, renewable energy sources are intermittent at the diurnal and seasonal scales, and are disparate in their geospatial availability. ESMs using classical modelling approaches (i.e. optimisation or simulation) typically increase the number of time slices, and/or implement clusters in order to capture time-dependent supply phenomena. They can also further disaggregate supply regions to account for the distribution of renewable energy resources. However, renewable supply characteristics still need to be introduced exogenously in most cases, requiring the mapping of the resource in an up-stream process.

New reanalysis data sets, derived mainly from long-term satellite earth observation, have made it possible to simulate the hourly fluctuations in power output from renewable technologies. However, studies with hourly resolution are typically limited in scope to a single, or a few years because of the difficulty in dealing with large data sets [34]. Another problem is the inter-annual variability of renewable generation which cannot be captured by a single year of wind data; wind capacity factors for a single calendar day can vary between 0% and 100% in a data series of 25 years [35]. Methods including heuristically selecting extreme days and then clustering remaining time periods can yield acceptable accuracy in high VRE scenarios when compared with a 1-hourly reference model [35,36].

Until recent times, most modellers have made crude estimates of the global wind resource because of the arcane principles of GIS analysis to the field of ESM modelling and the scarcity of high quality wind reanalysis data sets. The IEA's ETP model is built on the TIMES modelling framework [37], and for the first time in 2016 included analysis [38] of onshore wind energy potentials via a bottom-up, GIS-based, estimation of capacity potential per region. Other ESM modellers have made use of available data sets in the scientific literature for regional potentials. Loffler et al. [13] design a 100% renewable energy system for 2050 using the OSeMOSYS[1] modelling system [39]. They use land area deemed suitable for development by Archer and Jacobson [40] and a constant capacity density of 5 MW/km^2 from Arent et al. [22]. Hoogwijk et al. [41] produced global and regional supply curves by estimating the global economic potential of onshore wind energy which can be directly used by ESM modellers. Subsequently, several analyses and open databases have been developed to provide better quality renewable input data for the modelling community, e.g, *Renewables.ninja* [42], *OEDB*[2] [43] and *OpenEI* [44].

2.3. Geospatial modelling of offshore wind energy potentials

In recent years, the long-term operation of earth observation satellites has allowed the collection of global-scale data, including atmospheric variables. This has allowed the assessment, on a global scale, of wind energy potentials from a bottom-up perspective.

Detailed studies of offshore wind energy potentials have mostly focussed on country-level technical or economic assessments [45–48]. Among these country-level studies, the main focus is often finding suitable development sites based on wind availability and cost criteria [45,46,49], which are important insights for national-level energy system planning.

Several potentials analyses are also carried out by government and non-governmental organisations [21,38,50]. IRENA[3] publishes a wide range of renewables-related regional and global data for download via its Global Atlas for Renewable Energy, including the Denmark Technical University (DTU) Global Wind Atlas (GWA), which offers 30 km of offshore wind data. However, its main limitations for this application are, firstly that it only covers 30 km of offshore territory (out of 370 km of EEZ envelope); and secondly, although the spatial resolution is improved compared with NASA MERRA-2 data upon which it is based, the wind speed values are static in time and therefore are not suitable for distributing generation potential among model time slices.

The main limitation of regional or global offshore wind energy potential estimates is that they do not explicitly describe generation potential with respect to time steps or time slices, which is necessary for detailed energy planning. The importance of explicitly describing the generation potential by time can be seen in Archer and Jacobson [40] where they find that practical wind power resources are highly seasonal. Pfenninger [35] also shows that intra-annual variations can be significant and therefore simply using a single or a small number of years of wind speed data is not sufficient.

3. Data input

The basis for this study are the global wind speeds from the NASA MERRA-2[4] [51] reanalysis data set. It provides wind speeds with a spatial resolution of 0.625 × 0.5° (approximately 50 km at the equator), and 1-hourly temporal resolution with a data

[1] The Open-Source Energy Modelling System.
[2] OpenEnergy Database.
[3] International Renewable Energy Agency.
[4] The Modern-Era Retrospective Analysis for Research and Applications, version 2.

Table 2
List of raster and vector data sets used in this study.

Data set name	Description	Spatial resolution	Source
NASA MERRA-2	Global wind speeds (35 years of hourly wind speeds)	0.5° × 0.625°	Link [51]
DTU Global Wind Speed Atlas (GWA) – v.1	Global wind speed simulation model (averaged)	0.05° × 0.05°	Link [52]
GEBCO 2014	Global topography and bathymetry	0.008333°	Link [57]
Global Administrative Areas (GADM)	World country borders	vector	Link [58]
World Economic Exclusive Zones (EEZ)	Offshore marine areas	vector	Link [54]
World Marine Heritage Sites (WMHS)	Offshore protected areas	vector	Link [59]
World Database of Protected Areas (WDPA)	UNEP database of internationally recognised protected conservation areas	vector	Link [56]
TeleGeography Submarine Cable map	Global map of submarine cables and landing stations	vector	Link [60]

collection period of approximately 35 years (1980–2015). The DTU Global Wind Speed Atlas (GWA) [52,53] uses the WaSP wind simulation tool to generate high resolution wind speeds accounting for the microscale wind speed-up effects due to topography. It is calculated from over 30 years of NASA MERRA data, resulting in averaged wind speeds for the entire globe, including a 30 km envelope into open waters. Section 4.2.1 describes how the GWA data set is used in combination with the MERRA-2 data, in near-shore regions, to generate a bespoke wind speed data set for this study.

The remaining data sets are used to overlay wind data for masking and suitability consideration. Offshore wind analysis is carried out within the EEZ areas for each country [54,55], while heritage and protected areas are excluded from development. The World Database on Protected Areas (WDPA) [56] is the most comprehensive global database on terrestrial and marine protected areas. The 2014 General Bathymetric Chart of the Oceans (GEBCO) data set is the highest resolution and most up-to-date global ocean bathymetry data and its resolution is used as the basis for interpolating all the rasterised data in this study (see Table 2).

4. Methodology

4.1. Overview

The methodology used in this study can be described as a bottom-up approach, which characterises the capacity factor (CF) of offshore wind turbine operation by calculation of the energy content of the wind from high-resolution global wind speed data. Special attention is given to the wake losses using a simple empirical model from the literature. The available offshore surface area is limited to reflect bathymetry constraints and competing surface uses. A GIS approach allows the overlay of spatially coincident raster and vector data. The methodology is shown in Fig. 1 and can be summarised by the following steps. Appendix A shows a summary of all input parameters for this analysis.

1. Wind speed data calibration

NASA MERRA-2 wind speed data is bias-corrected and interpolated to a high spatial resolution using the DTU Global Wind Atlas (GWA). Section 4.2 describes the generation of the global wind speeds.

2. Produce global capacity factors (CFs)

A CF is assigned to each grid cell, and for each time slice, by combining a geographically specific wind speed distribution with turbine power characteristics. Array efficiency is applied to the capacity factor to account for the wake effects of multiple turbines in close geographic proximity.

3. Calculate global wind energy generation potential

Capacity is considered in each grid cell with respect to the suitability of the surface area and water depth constraints for current technologies. Availability due to operation and maintenance (O&M) constraints are factored. Finally, local generation potentials of wind farm arrays are summed from wind farm capacity density and CF for each grid cell.

4.2. Calibration of wind speed data

In previous studies, wind speed resolution (temporal and spatial) is cited as a major source for error in the calculated power output potentials [52]. In open source databases, detailed representation of wind speeds is not available. Therefore, in this study, two data sets are combined and calibrated to yield the best spatial and temporal resolutions.

This study makes use of the *Renewables.ninja* model [42,61], a software platform which simulates the power output from wind farms based on historic wind speeds for every grid location from the NASA MERRA-2 data set. It is used here to take the provided hourly wind speeds and convert them to turbine outputs using real turbine power curves. The underlying wind speeds are validated in Staffell & Pfenninger [61].

4.2.1. Bias correction of wind speed data

NASA MERRA-2 wind data are bias corrected using the GWA data set, as it has the best spatial accuracy available. GWA is a micro-scale, simulated wind speed data set using MERRA-2 as its input, and its spatial accuracy is validated in Ref. [52]. Fig. 2 shows graphically the difference between the two data sets. In the left panel, the long-term average wind speed from MERRA-2 data can be seen, with wind speeds ranging between approximately 7-12 m/s. The GWA (right) can be seen to capture variations close to the shoreline much more granularly; wind speeds as low as 4 m/s can be identified. However, the data only cover an area reaching 30 km away from the coast [52].

The calibration is achieved via time-invariant linear scale factors at each location, so that the temporal properties of the MERRA-2 data are preserved, but wind speeds are corrected and interpolated towards the more accurately characterised long-term mean GWA wind speed. Fig. 3 shows a graphical depiction of Denmark's EEZ wind speeds, comparing average MERRA-2 wind speeds to the GWA wind speeds within the GWA envelope. A linear regression of the two data sets for each country yields a multiplication factor by which all MERRA-2 wind speeds are adjusted. This relatively simple approach provides an improved calibration whilst protecting against the influence of extreme outliers, accounting for the high variability of wind speeds near to shoreline in each disparate territory.

4.2.2. Time slicing of wind speed data

To estimate the capacity potential on a global scale, only an aggregated set of data is used. The hourly, high resolution wind

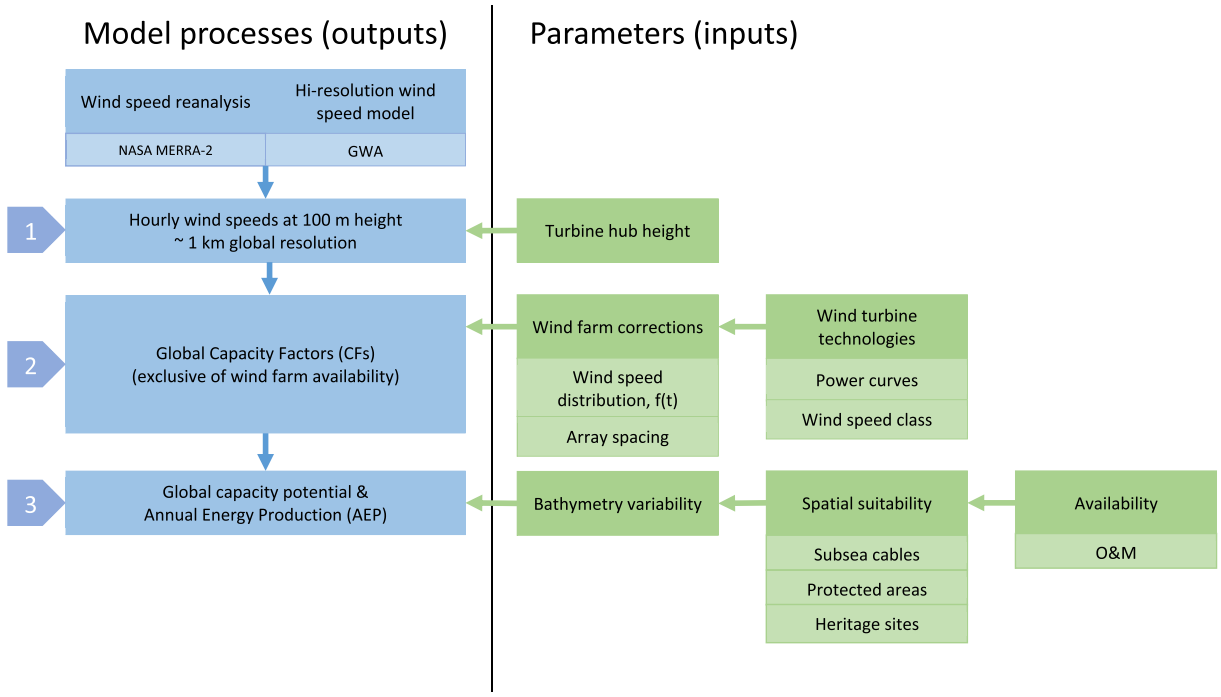

Fig. 1. Diagrammatic outline of the study's methodology. Intermediate model outputs (blue), are in the order of the programmatic process flow. Collected or calculated input parameters and variables are in green. (For interpretation of the references to colour in this figure legend, the reader is referred to the Web version of this article.)

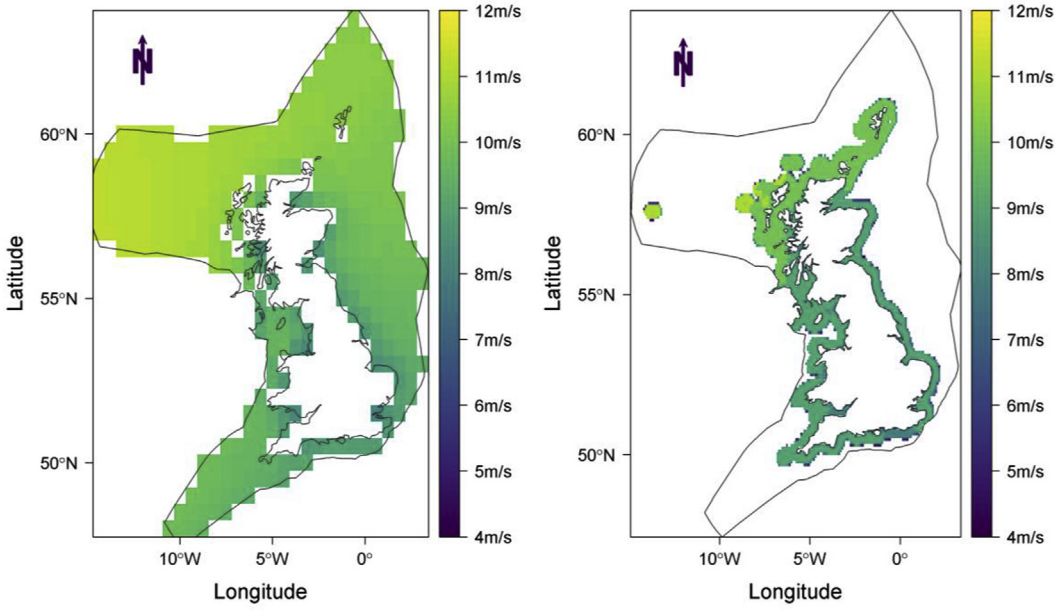

Fig. 2. Long-term average wind speed magnitudes from the raw NASA MERRA-2 reanalysis data set (left) and the DTU Global Wind Atlas (right), within the United Kingdom Economic Exclusive Zone. The DTU dataset only covers 30 km distance away from the coast. The resolutions are $0.625 \times 0.5^{\circ}$ versus 0.01×0.01, respectively. The DTU data use frequency-weighted averages from over 30 years of NASA MERRA-2 input data, improved with micro-scale wind speed simulation modelling.

speed data generated by the wind speed model (described in section 4.2) is derived from 35 years of NASA MERRA-2 reanalysis data, and as a result contains several Terabytes (TB) of raw data. To retain the seasonal and diurnal variations of the wind resource while creating data suitable for most ESMs, this data is binned into 32 time slices. Each slice represents the full time series of data, where values for each sub-day time slice are averages from all the years covered in the data. Each season corresponds to a quarter of the year rather than the climatic seasons of a specific region (i.e. January–March, April–June, etc.). Table 3 summarises the time slice definition used in this study.

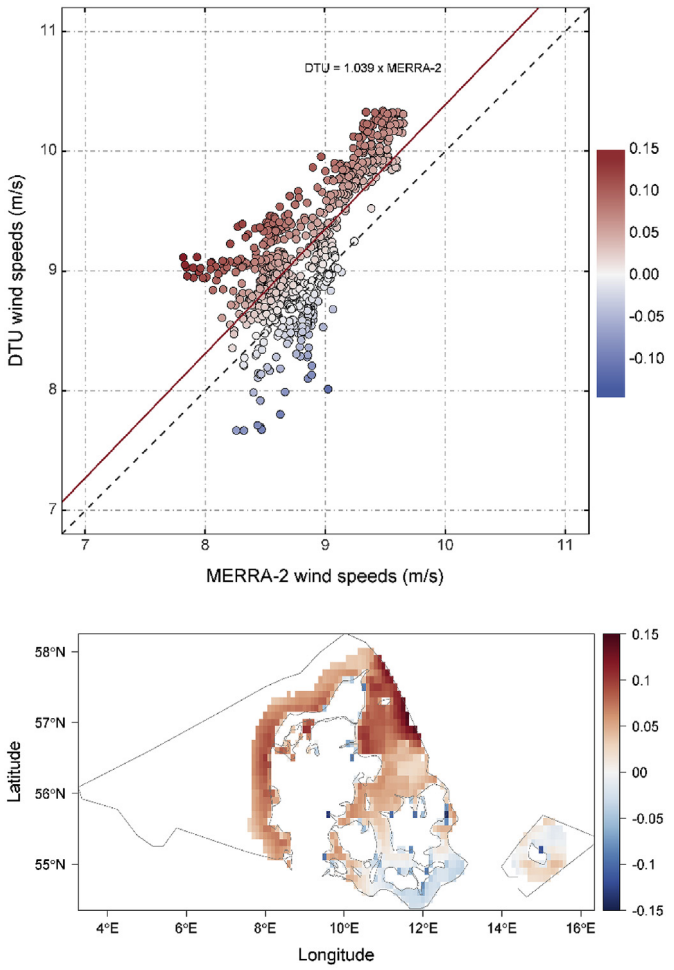

Fig. 3. A comparison of coincident DTU data and MERRA-2 data (spline-interpolated) for Denmark via a calibration factor (−0.15 - 0.15). A linear regression shows that DTU predictions are higher than MERRA-2 predictions at higher average wind speeds. At lower speeds, the DTU data show much higher variability since the spatial variance is captured more accurately. This regression is used for the time-invariant bias correction and interpolation of the MERRA data for this analysis.

Table 3
Time slice methodology used in this study. 32 time slices represent 4 seasons and 8 diurnal time periods per representative season.

Time slice level	Number of bins	hours/bin
Seasonal	4	2190
Diurnal	8	273.75
Total	32	8760

4.3. Capacity factors

To yield realistic wind farm energy production estimates, the wind speeds for each grid location are converted to capacity factors (CFs), considering the wind speed distribution suitable for each grid location. Because of the cubic response of the turbine power curve, and the calibrated wind speed distribution provided by the *Renewables.ninja* model, CF is approximated by the multiplication of these distributions divided by the nominal turbine power for each class of turbine, leading to capacity factors for 2 classes of turbine (see section 4.3.1). A detailed explanation of this derivation can be found in the supplementary material, section 1.2.

Table 4
Wind speed classes consistent with International Electrotechnical Commission specification [62]. The wind class of each turbine is allocated as I, II or III based on its rated power density, as specified in last column of the table.

IEC wind class	Annual average wind speed (m/s)	Power density (W/m^2)
III	≤7.5	300–350
II	≥8.5	350–450
I	≥10	>450

4.3.1. Wind speed class

Wind turbines are designed for the specific conditions they will endure at the installation site. This means the electrical generator, rotor and turbine are optimised for the wind speeds they are most likely to encounter. Different turbine models therefore cater for specific wind speed classes, where the class is related to the annual average expected wind speed.

Since a range of wind turbines is considered in this study, only the most suitable class of turbine is assumed to be deployed in each grid cell. The average wind speed for each grid cell is derived from the long-term average of the MERRA-2 global wind data, because it extends beyond the 30 km envelope of the GWA. It is interpolated to the required resolution (1 km × 1 km) using bilinear interpolation. The wind speed class of each turbine is determined by considering its power density. Table 4 summarises the wind speed classes as defined by the International Electromechanical Commission, and the corresponding range of power density for turbines of that class. For turbine specifications and a detailed derivation of capacity factors for each class, see supplementary material, sections, 1.3 and 1.4.

Fig. 4 shows the wind conditions in the EEZ areas of Europe (left panel). The right panel shows how those wind conditions lead to the allocation of either class III or class II turbines. Large areas across the Mediterranean, and close to shorelines in northern Europe are typically suitable for class III turbines (i.e. lower average wind speeds), and more northern areas are suited to class II and above.

4.4. Calculation of energy generation potential

The capacity potential of offshore wind depends not only on the local treatment of wind speeds and capacity factors, but also on array characteristics, geographical constraints, and downstream losses.

An exemplary wind farm of array size 10 × 10, with a spacing of 10 rotor diameters is assumed, leading to a capacity density of 3.14 MW/km^2 for an exemplary 5 MW wind turbine. This array size and spacing leads to a constant array efficiency of 88.55%, which is applied to the capacity factor for calculation of the final generation potential in each grid square. An explanation of these choices and the derivation of array efficiency can be found in the supplementary material, section 1.2.

4.4.1. Offshore spatial constraints

Offshore constraints need not consider urban and rural land uses. However, there exists a genuine opposition to placing wind farms within the visible horizon of the coast, mainly because of the visual impact. In the Netherlands, it is prohibited to build wind farms within Territorial Waters, i.e. within 12 nautical miles (22 km) of the coast [63]. In the UK too, the latest round of tenders for wind farm development explicitly prefers sites beyond this 22 km zone due to the government's strategic environmental assessment [64]. In this study, the 0–10 km region (approximate visible range) around the coast is assumed a separate category; nevertheless, potentials are still calculated for this area.

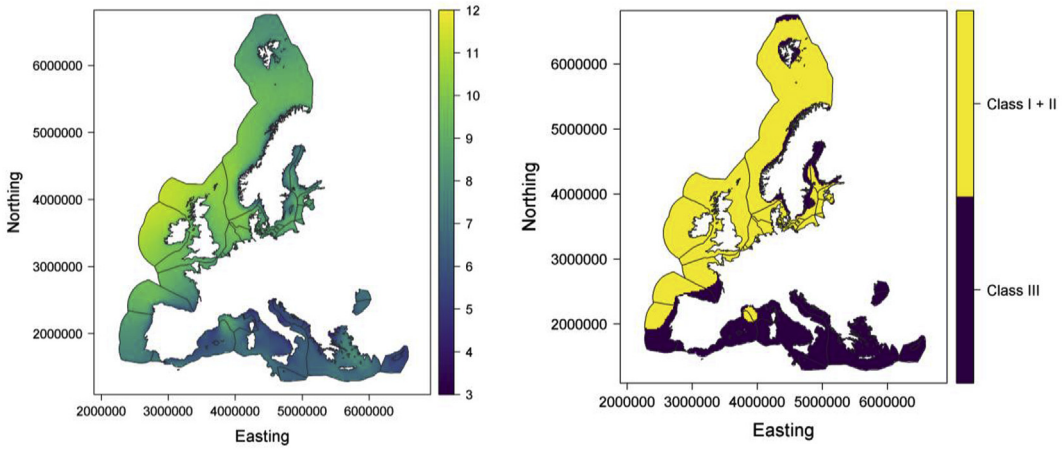

Fig. 4. Map of average wind speed (m/s), left, and suitable winds speed classes (right) within the Economic Exclusive Zones of Europe. Based on long-term average wind speeds (from 35 years of MERRA-2 hourly data), the spatial extent of each suitable wind speed class is from Table 4. I.e., average wind speeds below 8 m/s are classified Class III and those above 8 m/s are classified II and I.

An important constraint in the planning of offshore installations is their disruption to existing offshore activities. For example, hot spots on major commercial shipping routes may restrict wind farm development from happening in certain areas. However, aggregated and historical data from the Automated Identification System (AIS) are only available from commercial outlets, with some open-source country-scale data available from national governments; for example, for UK [65,66] and European [67] waters. At this time, however, no global data set is available that derives vessel type and density at a suitable spatial resolution.

Table 5 summarises the remaining constraints imposed for this study. Development is only allowed within the Economic Exclusive Zones of each country. This includes an area off the coast of each country's shoreline that stretches a maximum of 200 nm (370 km) away from the coast. Furthermore, in the EEZ boundaries data set [54,68], the list of boundaries consists of 239 areas, which is possible because some areas are designated across multiple countries. In order to avoid undercounting the potential for each country, those duplicated EEZ areas were counted for both countries named in the "country" attribute field. Therefore, the sum total of areas included in this study is more than the total area in reality, by approximately 140,000 km^2 or 0.1%.

Secondly, it is assumed, from the availability and maturity of offshore foundation and installation technologies, that the deepest areas available for foreseeable development will be 1000 m. This depth limit is also used in recent analysis [15], making results directly comparable. It can be seen in Fig. 5 that although the total area within the EEZs of European countries appears large, the areas with significant resources under 1000 m is much smaller. Fig. 5 (right) shows a categorical depiction of water depth in Europe, demonstrating the extent that each foundation technology could feasibly be deployed with current technologies.

The water depth of planned wind farm sites is an important consideration because the costs and capabilities of different technologies varies widely. Table 6 shows the water depth categories chosen in this study based on an assessment of current technologies. Several foundation technologies range in feasible installation depth between 0 and 60 m. Beyond 60 m, floating (or buoyant) foundation technologies are the only economically feasible option. For each category, outputs of this study are presented according to these water depth categories.

Finally, the TeleGeography Submarine Cable map of currently operating undersea cables is available for the whole globe. Because of the high cost of damaging these cables and the risk of damage due to installation vessels and machinery, an approximate buffer of 1 km either side of each cable is excluded for development (i.e. a suitability factor of 0%).

4.4.2. Availability factor and other losses

Not all of the potential energy generated by wind farms can be fully realised in reality. Depending on the age of the wind farm [69], its size, and the conditions it endures, operation of turbines within a farm must be periodically halted for maintenance (Operations & Maintenance). This study uses 97% as a multiplying factor for the potential wind farm output. This figure is higher than in comparison to other studies [15,17,18,22], but is in line with recent industry experience, as surveyed by Bloomberg New Energy Finance [70]. In their analysis 73% of O&M contracts had an energy-based availability of 97% and more than 15% had a guarantee of 98%.

No account of losses due to electrical transformation or transmission are included. Only the output of the wind farm is considered rather than electricity available at grid level.

4.4.3. Study outputs

The results in this study will be presented firstly as global energy generation potentials with respect to a number of important

Table 5
Suitability factors for offshore areas.

Constraint	Data set	Suitability factor
Economic Exclusive Zones	EEZ union data set	0% (outside of zone)
Protected areas	World Marine Heritage sites	0%
	World Database on Protected Areas	0%
Vicinity of subsea cables	TeleGeography Submarine Cable map	0%
Water depths > 1000 m	GEBCO	0%

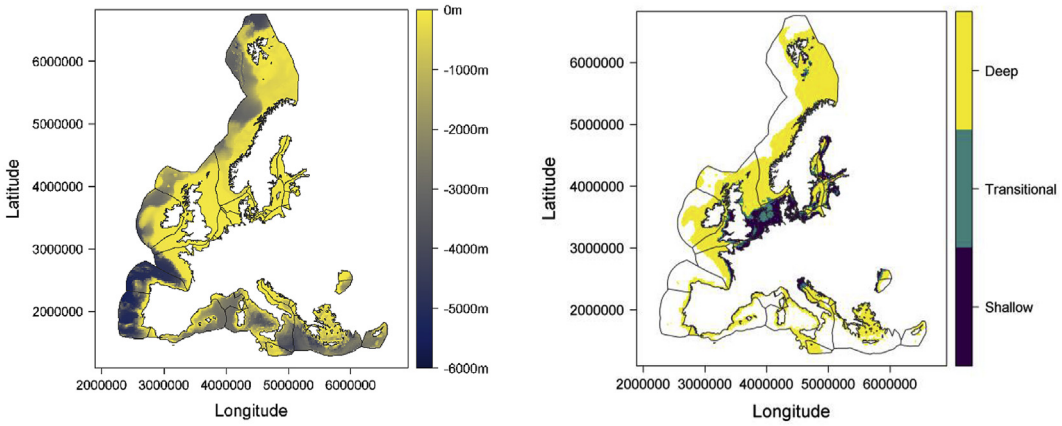

Fig. 5. Water depth around Europe, within the Economic Exclusive Zones (left); categorical depiction of water depth (right). Each depth category is suitable for installation of different turbine foundation types: Shallow areas (0–40 m) are suitable for Monopiles; Transitional (40–60 m), tripod or jackets; and Deep (60–1000 m), floating. White areas within the EEZ boundaries are deeper than 1000 m, and therefore deemed out of the scope of foreseeable development.

Table 6
Water depth categories used in this study and suitable foundation technologies.

Water depth range (m)	Water depth category	Suitable foundation technologies
0–40	Shallow	Monopile, Mono-bucket (suction bucket), Multi-pile (tripod and jacket)
40–60	Transitional	Multi-pile, Gravity Base Structure (GBS)
60–1000	Deep	Floating

parameters. Fig. 6 shows a series of schematics of the UK to demonstrate how the extent of the spatial constraints imposed could affect the electricity generation potentials. Panel (a) shows the loss of area potential due to known protected areas (WDPA) and submarine cable locations. Panel (b) shows the extent of the depth categories chosen for this study. Panel (d) shows the distance categories. It can be seen that in both of these cases, and without considering the excluded areas already considered, large parts of the EEZ are not included in the energy potential calculation due to the upper bounds of both variables being chosen to reflect current feasibility of foundation technologies and transmission lines, respectively. Panel (c) shows areas of average annual capacity factors, showing how distributed different tranches of capacity could be when implemented in an ESM.

5. Results and discussion

Results firstly focus on global average energy generation potentials (averaged from 35 years of wind speed data) for each country. Potentials are presented with respect to distance to shore and water depth, and finally considering the top quarter (25%) of the highest quality wind available in each country's EEZ. Energy generation potential at three depth categories and four distance categories are produced. From these results, comparison can be made to other global and country-level studies that provide energy potentials for offshore wind (see sections 5.1.3 and 5.1.4). Quantitative results are available as supplementary data in the online publication (see section 7).

5.1. Global offshore wind potential

The global offshore wind potential is presented for 157 countries with a viable offshore potential, i.e. connected to a shoreline and possessing average capacity factors over 20%.

5.1.1. Global results

Fig. 7 summarises the generation potential for a number of high potential countries, including Australia, Norway, Indonesia, and Argentina; countries with both large relative offshore areas, and high average wind speeds and capacity factors.

The generation potential is the sum, over all allowed areas, of the installed capacity density multiplied by the capacity factor, averaged over 32 time slices. Fig. 7 shows the total generation potential for shallow (0–40 m), transitional (40–60 m) and deep (60–1000 m) depth categories, with a point overlay showing the total electricity demand of each country in 2015 [71]. For many countries, the offshore wind generation potential could provide the total electricity generation for the whole country. In the UK, 302 TWh of electricity was generated in 2015, while over 6000 TWh could be produced if all feasible areas of the EEZ were developed for wind energy. In Norway the total production of power was 110 TWh while the offshore generation potential is two orders of magnitude higher at 15,569 TWh.

A higher relative potential in shallow and transitional categories would indicate a more economically feasible. For example, Indonesia has over 2000 TWh of shallow water potential, and also 2000 TWh within near to shore limits (Fig. 8), indicating that Indonesia has favourable conditions for affordable offshore development. Conversely, Norway has a huge relative potential with respect to its total energy consumption, but almost all of its potential is located over deep waters (60 m+), with less than 1000 TWh available in shallow and transitional depths, combined.

Fig. 8 shows the generation potential by distance to shore. These figures give an indication of how much potential exists relative to approximate transmission distances. The generation potential is divided into four categories; <10 km (unlikely development), 10–50 km (near to shore), 50–100 km (intermediate), and 100–200 km (far from shore).

Large potentials in the 10–50 km range would indicate significant scope for economically feasible wind farm development. Australia, Norway, China, Brazil, and Japan have vast relative

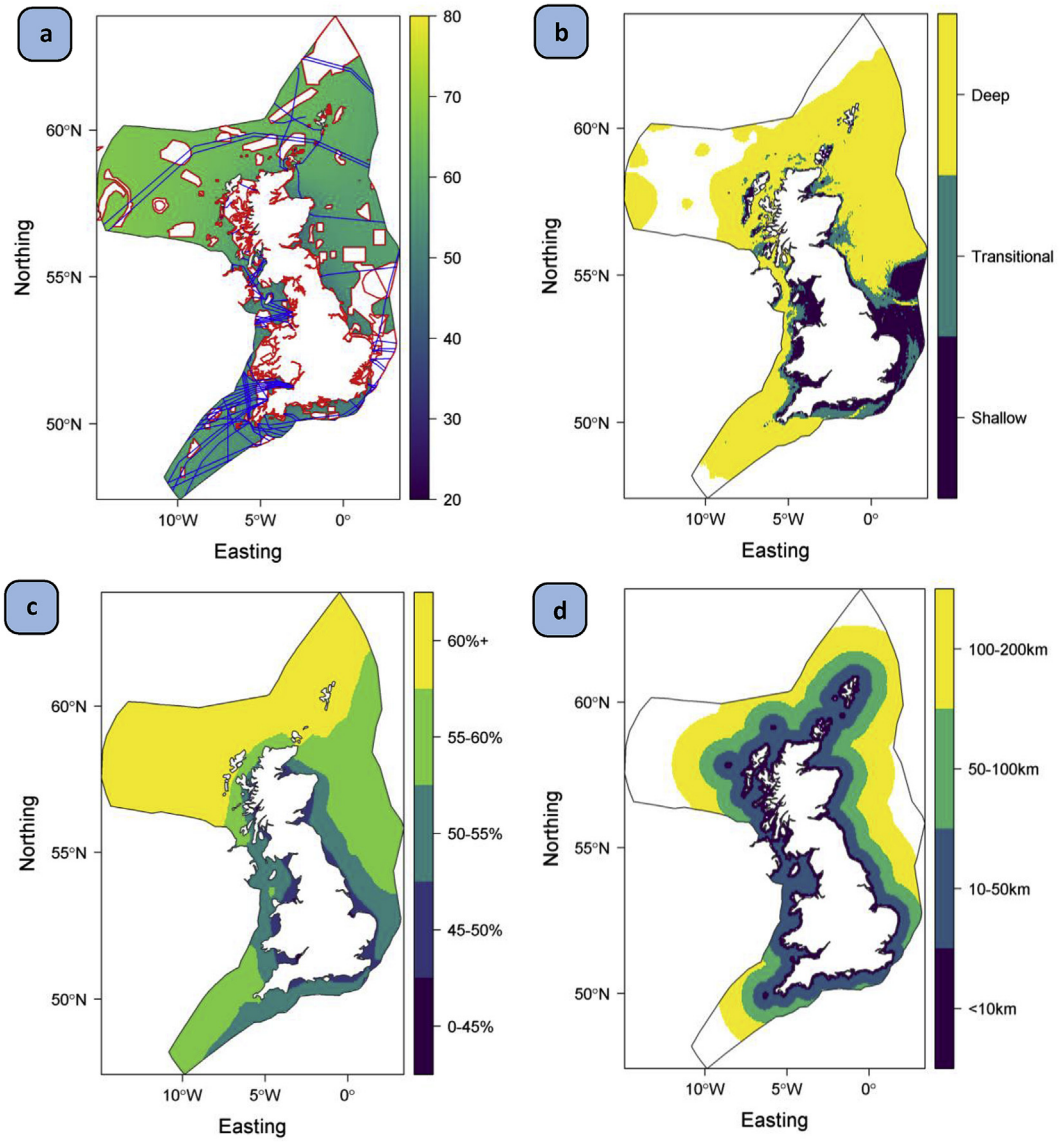

Fig. 6. A graphical depiction of the United Kingdom (UK) Exclusive Economic Zone (EEZ) and its spatial constraints for offshore development. The top left panel shows mean capacity factors (%) of the UK EEZ, accounting for placement of wind class II and III turbines. Infeasible areas are highlighted in red and blue, namely: World Database on Protected Areas and undersea cables, respectively. Approximately 1 km either side of the blue lines are excluded. The remainder of the panels show the output categories of this study. Outputs are available with respect to (b) depth categories, (c) capacity factor tranches, and (d) distance from coast. For (b) and (d) the full capacity/generation potential of the whole EEZ is not available due to the upper bounds chosen for each constraint, i.e. white areas are not counted. (For interpretation of the references to colour in this figure legend, the reader is referred to the Web version of this article.)

potentials in this near to shore category. Australia generated 252 TWh in 2014–15 [72], and the offshore potential just in this near to shore area is over 6000 TWh. However, in this analysis, there is no consideration of how far from grid connection these potentials are, especially relevant for remote regions.

5.1.2. Regional results

Table 7 shows a summary of the world offshore wind energy potential, aggregated into world regions as defined by the UN "sub-region" definition. The first row named "No allocation" contains world territories with no obvious sovereign designation, e.g. French Southern Territories, etc.

Northern America and Eastern Europe have the largest overall capacity potential, but Eastern Europe has a much higher proportion of its generation potential in shallow and transitional waters. Globally, the vast majority of the potential is in deep waters with 230,004 TWh/year, but there still exists 64,845 TWh/year in the most accessible (shallow, 0–40 m) waters.

5.1.3. Comparison to global results

Table 8 shows a comparison between this study and other studies that produce estimates for global offshore wind potentials. This study finds a global offshore resource of 329,600 TWh per annum. This AEP potential is disaggregated with respect to water depth, which is the approach other studies have taken. At the depth ranges shown, this study finds considerably more resource than some comparable global studies, but it is more modest than regional studies (as shown in the following section).

The NREL [22] and Harvard [18] study are similar in methodology, with the only difference in output being due to the assumed turbine power density, which would otherwise lead to more similar results. There are several differences between this and those

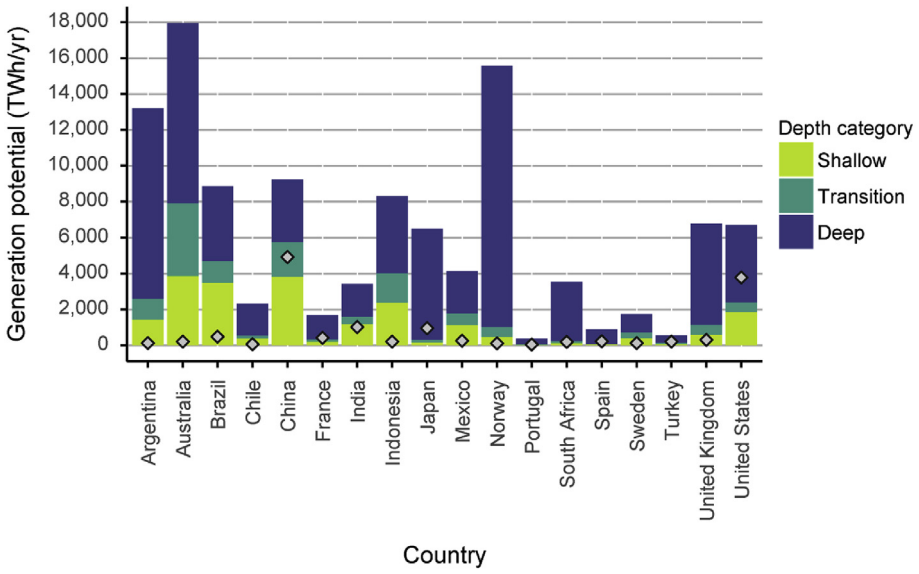

Fig. 7. Annual average energy production (AEP) potential of offshore wind farms for different depth categories for a selection of high producing countries (shown in alphabetical order). Depth categories are Shallow (0–40 m), Transitional (40–60 m) and Deep (60–1000 m). The estimated AEP is the average generation over all time slices, summed over all feasible areas of the country Exclusive Economic Zone, up to the prescribed depth limit. The overlaid point on each bar is the electricity generation in 2015 from Ref. [71] for comparison.

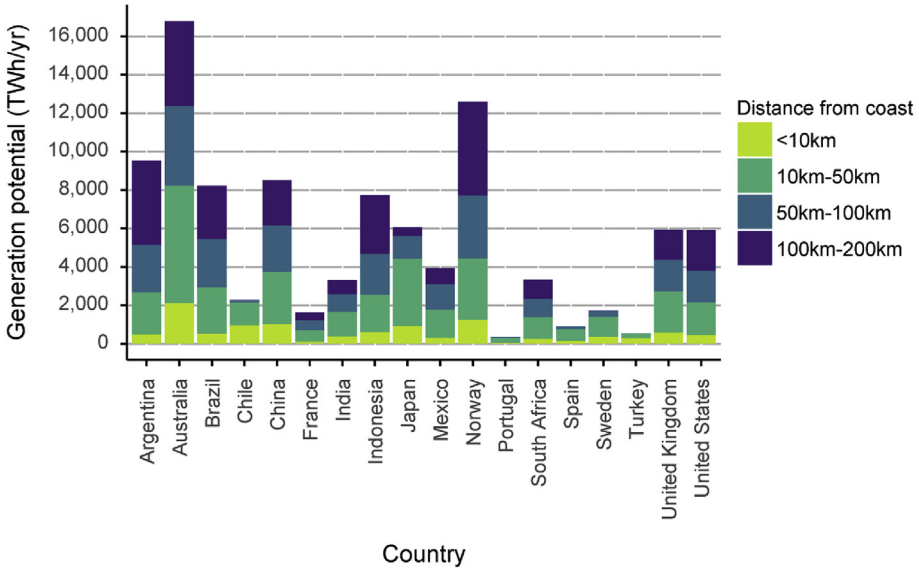

Fig. 8. Annual average energy generation potential of offshore wind farms for different distance categories for a selection of high producing countries (shown in alphabetical order). The data presented only shows potentials that lie within the specified distance category; many countries have potentials beyond the 200 km limit but within the 200 nautical mile (370 km) limit of the Exclusive Economic Zone.

studies:

1. The power density is lower at 3.14 MW/km^2 versus 5–5.84 MW/km^2. This lower turbine packing density comes from the use of a 5 MW, 126 m rotor diameter turbine, with 10 RD spacing, which exceeds the 8RD spacing and 3.5 MW used in those studies;
2. This study includes areas with a water depth up to 1000 m rather than 200 m;
3. This study includes the potential of the whole EEZ area up to 200 nm (370 km) instead of the 100 nm (185 km) limit used in those studies;
4. The resolution of atmospheric data used in those studies was 2.5° × 2°, while in this study, the MERRA-2 data set used is 0.625 × 0.5 and calibrated with the 0.05° × 0.05° DTU GWA. The DTU validation literature show over several geographies that the wind power density can increase by several factors by capturing micro-scale speed-up effects [52].

Archer and Jacobson [17] only provides total potential for onshore and offshore areas combined, but they state that potentials are found for the entire globe with 71% of areas covered by water, and that wind speeds were found to be 90% higher in offshore areas, on average. Since the wind speed data came from a relatively sparse

Table 7
Summary of regional potentials, by UN definition of sub-region. Feasible Capacity potential is in the first column, with the generation potentials of several categories of capacity calculated based on annual average capacity factors.

Region	Average CF (%)	Capacity (TW)	AEP Shallow (TWh)	AEP Transitional (TWh)	AEP Deep (TWh)	AEP Top 25% (TWh)	Total AEP (TWh)
No allocation	53%	0.02	3.9	0.4	74.9	6.0	79.2
Australia and New Zealand	48%	7.29	4340	4390	19,100	4380	27,800
Caribbean	43%	1.24	1640	152	2360	658	4150
Central America	32%	1.97	2090	846	3510	1580	6450
Eastern Africa	38%	2.10	1860	681	4650	1920	7190
Eastern Asia	41%	5.53	4670	2750	12,800	4950	20,200
Eastern Europe	43%	16.80	18,700	9590	40,300	15,100	68,500
Melanesia	37%	1.29	1030	306	2850	1110	4190
Micronesia	32%	0.26	241	99.4	498	316	839
Middle Africa	67%	1.11	146	90.1	6260	6430	6490
Northern Africa	35%	1.78	893	533	4160	942	5590
Northern America	46%	16.80	8880	4360	52,900	12,800	66,200
Northern Europe	54%	7.77	3110	2320	32,600	13,400	38,000
Polynesia	35%	0.45	213	38.8	1250	668	1500
South-Eastern Asia	28%	7.02	5430	3550	10,300	2860	19,300
South America	44%	7.06	7150	3200	19,900	7860	30,200
Southern Africa	47%	1.42	149	137.0	5560.0	3350.0	5850
Southern Asia	29%	1.99	1940	689.0	2640.0	628.0	5260
Southern Europe	33%	1.71	304	221.0	4630.0	1650.0	5150
Western Africa	32%	0.18	204	51.3	321.0	149.0	576
Western Asia	28%	1.23	933	320.0	1970.0	612.0	3230
Western Europe	53%	0.63	918	553.0	1370.0	1860.0	2840
Totals	–	85.64	64,845	34,878	230,004	83,229	329,584

Table 8
Summary comparison of global average offshore wind energy potentials with main constraints and water depth categories reported where available.

Author	Resource constraints	Power density (MW/km^2)	Offshore wind energy potential (TWh)			
			Shallow (0–20 m)	Transitional (20–50 m)	Deep (50–200 m)	Total
NREL[a] [22]	<200 m depth 10% array losses >20% avg. CF	5	14,200	51,300	100,300	192,800
Harvard [18]		5.84	42,000	40,000	75,000	157,000
Archer and Jacobson [17]	≥6.9 m/s (≥class III)	9	–	–	–	630,720
Dupont [15]	≥8 EROI constraint Within EEZ <1000 m depth	6.4	–	–	–	211,667
This study	<1000 m depth 12.5% array losses >20% avg. CF	3.14	64,800 (0–40 m)	34,800 (40–60 m)	230,000 (60–1000 m)	329,600

[a] United States National Renewable Energy Laboratory.

number of samples, and the turbine sizes are relatively small, the result from this study is almost definitely very conservative.

Dupont et al. [15] conduct a careful study in which the global offshore wind energy potential is constrained not only with bottom-up constraints, including a depth limit of 1000 m (the result shown in Table 8), they also place a constraint on energy returned for energy invested (EROI); that is, the minimum energy delivered over the life time of a wind farm as a fraction of the energy resources invested, and set to a minimum of 5, 8, 10 and 12. Physical constraints are similar to this study with protected areas and depth limits identical. However, the average installed capacity density was just 2 MW/km^2, with a corresponding array efficiency of 82%, due to an optimisation process that chose variable turbine packing density to maximise net energy production per 0.75° x 0.75° grid cell. These low average capacity densities over such large grid cells could in this case be a limiting factor.

5.1.4. Comparison to country studies

Table 9 shows a summary comparison of this study's results to a number of country level offshore wind energy estimates. The European result [21], conducted by the European Environment Agency, is the only case which produces a lower generation potential. Only depths up to 50 m were considered which explains some of the discrepancy. However, they present future offshore potential for 2030, assuming that capacity density increases to 15 MW/km^2, with 90% array efficiency, which leads to a large capacity potential relative to the generation potential.

In comparison to the other country studies, this study only produces modest estimates for capacity and generation potential. In the USA study, this discrepancy can be explained with two main differences; firstly, potentials were calculated for average wind speeds above 7 m/s, with no restrictions to spatial suitability. In this study, only 28% of the EEZ was available after protected areas, submarine cables, and depth limits were imposed. Secondly, an assumed, constant energy density of 5 MW/km^2 was used compared to 3.14 MW/km^2 in this study.

The UK study [45] assumes an exemplary wind farm of 1.28 GW (256 turbines) located in each 10 km × 10 km grid square, leading to an installed energy density of approximately 12.8 MW/km^2, with 11% array losses, which would be inconsistent at such a packing density. The entire EEZ was available for development with no depth restriction. The allowable area is not available from that study, but in this study we find only 59% of the UK EEZ is available for development after protected areas and depth zones are removed.

In Nagababu et al. [46] (India) capacity density is not available, but they do disaggregate areas by wind power density to yield average power output of an exemplary turbine. Three factors in this study lead to a high generation potential however. Firstly, the inclusion of the whole EEZ with no depth or distance limit. Secondly,

Table 9
Offshore wind potential comparison to country studies for Europe, the United States of America (USA), the United Kingdom (UK), and India.

Country/region	Resource constraints	Power density (MW/km^2)	Capacity potential (GW)		Generation potential (TWh/yr)		Author
			Author	This study	Author	This study	
Europe	<50 m depth 1 km minimum distance to coast	10	11,250	8939	30,000	39,361	EEA [21]
USA	>7 m/s	5	4150	2079	–	6704	NREL [50]
UK	LCOE < £160/MWh	12.8	7889	1341	11,963	6779	Cavazzi and Dutton [45]
India	40% excluded area for conflicting uses	–	2898	1282	15,230	3427	Nagababu et al. [46]

the use of an average capacity factor that does not account for the wind conditions at each grid point. And thirdly, the use of OSCAT satellite data which only provide data at 50 × 50 km spatial resolution, and temporal resolution at the order of days. Fig. 9 shows the energy generation density of India using the capacity coverage and capacity factors from this study, which lead to an annual generation potential of 3427 TWh/yr.

5.2. Outputs for energy systems models

The principle output for this paper is in the form of tranches of usable capacity for direct use in energy systems models. For most models, the "building" of capacity commences in a merit order, where the lowest cost, or highest quality, resource is built first. For this reason, the available capacity is binned into tranches with annual average capacity factor increasing in 5% steps. Capacity potential is produced for every country, for 32 time slices and for 12 average capacity factor tranches, so that energy system models can yield energy generation per time slice for various average capacity factors.

5.2.1. Capacity potential

Capacity potential results are visualised in Fig. 10 for several high capacity. Capacity is available for annual average capacity factors above 20%. The 12 capacity factor tranches are aggregated to four bins in Fig. 10.

Several countries have significant capacity potential above 50% average capacity factors, even while spatial constraints reduce the total EEZ area available. India has large area to exploit for capacity, but the most common capacity factors are in the range 20–40%. In contrast, the UK has very high average capacity factors, meaning it can exploit the relatively small EEZ in comparison to some of the large countries. In terms of capacity, Canada, Russia, Australia, Indonesia, the United States and Brazil have the largest offshore capacity potentials.

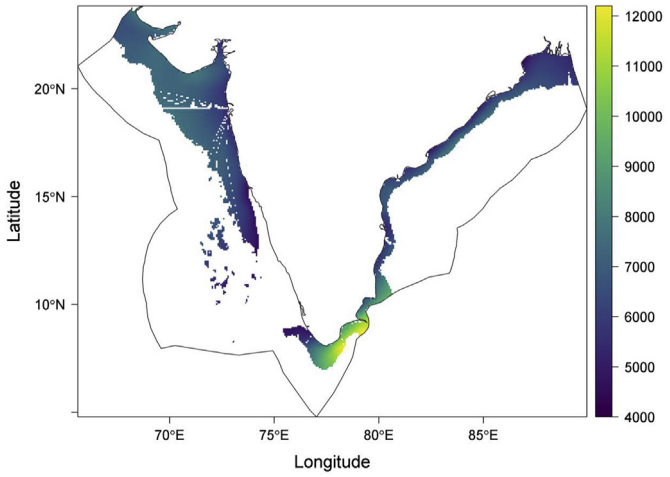

Fig. 9. Energy generation potential of India (MWh/km^2/year) with depth limits imposed and protected areas and subsea cable areas excluded.

5.2.2. Temporal phenomena

Temporal phenomena are introduced in this study via 32 time slices at the seasonal and diurnal scales. These are useful inputs for energy systems models because capacity can be deployed where demand coincides with high generation potential. The capacity potential in each grid square is exposed to a location-specific average capacity factor for each of 32 time slices. The seasonal and intra-day generation potential can therefore be assessed.

Fig. 11 shows the seasonal variation of energy generation for several high capacity potential countries. In northern hemisphere countries, the largest generation potential is between January and June (Winter-Spring), which is consistent with weather observations, equivalent to Jul–Sep in southern hemisphere countries.

Fig. 12 shows electricity generation of China's offshore capacity potential for each daily time slice, disaggregated by season. The diurnal generation profile for each season dips in the afternoon until late evening (14:00–23:00). However this pattern is largely mitigated by including the whole China EEZ area, since areas that experience a fall in wind power are offset by other areas experiencing a peak. Furthermore, as observed in Fig. 11, there is an obvious difference between time slices from different seasons. July to December experiences the lowest turbine generation, while January to June is the windiest period.

5.3. Testing limits to capacity density

If turbines are placed in arrays larger than 10 × 10, wake effects will significantly reduce the generation potential of each turbine. For this reason, it is not realistic to expect large portions of a country's EEZ to be developed. To understand the effect of the implicit addition of a buffer zone around each wind farm, the AEP potential of the United States of America (USA) is investigated.

Fig. 13 shows a representation of a square wind farm array with dimensions *a* x *a* and a buffer zone around the perimeter of width *b*. In the previous analysis, potentials were calculated by the summation of energy density per grid square, with an assumed array efficiency that corresponded to an array size of 10 × 10 turbines with an average spacing of 10 RD. If a buffer area around this exemplary wind farm is chosen such that turbines cannot be seen over the horizon from each other, the buffer width for each wind farm array should be approximately 5 km - a total of 10 km between arrays. The new capacity density over the extent of the investigated area is then:

$$\rho_n = \rho \times \frac{a^2}{(a+2b)^2} \#1$$

where ρ_n is the new wind farm capacity density and ρ is the initial capacity density. *a* and *b* are the widths of the wind farm and the

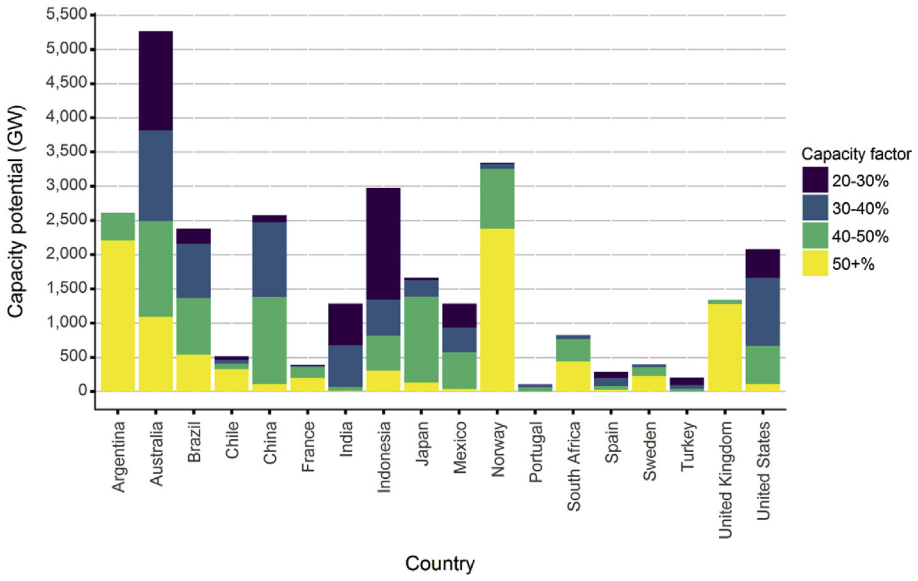

Fig. 10. Capacity potential for a range of high potential countries with respect to average annual capacity factor. For offshore wind, as opposed to onshore wind, capacity factors over 50% are common, and several countries have significant potentials above 30%.

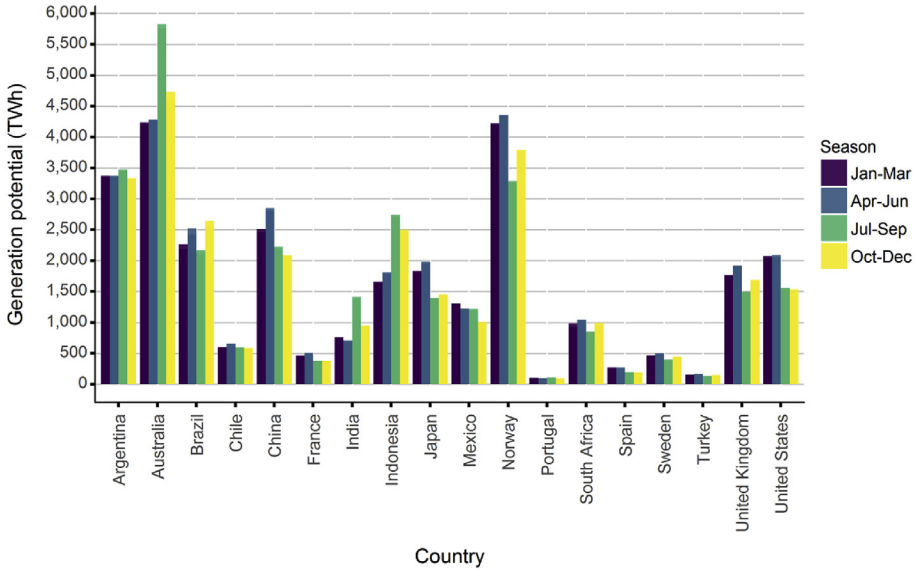

Fig. 11. Seasonal variation of offshore generation potential for several countries with high capacity potential. Since the data are produced with consistent time slices over the entire globe, the 4 seasons are defined as 4 quarters of the year rather than adjusted to suit the seasons of any one region.

buffer zone, respectively. For the exemplary wind farm with turbines of 126 m rotor diameter, with 10RD spacing, and an initial energy density of 3.14 MW/km^2, the new energy density is 0.97 MW/km^2.

Fig. 14 shows the offshore wind energy density of the USA, recalculated to include an average wind farm buffer size of 5 km. The energy generation density per annum ranges between 1690 and 5400 MWh/km^2/year, leading to an energy generation potential of 2065 TWh compared with the 6740 TWh calculated in the main results. The capacity potential becomes 640 GW compared to previously 2079 GW, or the 4150 GW calculated by NREL [50]. Therefore, if wind farms were to be deployed over large portions of a country's EEZ, the upper limit of the total generation potential would be severely affected by accounting for the spaces between adjacent wind farms.

6. Conclusions

This paper provides new insight into the available and exploitable offshore wind energy potential within each country with a viable offshore wind resource. The potential of offshore wind is temporally explicit so that researchers and policymakers are able to assess the offshore wind deployment potential against other time-variant factors critical to energy provision, such as electricity demand, weather variability, etc. The primary output is capacity potential for each country, disaggregated by time slice and annual average capacity factor, so that energy systems models may use the data directly.

Capacity potential was firstly restricted geospatially using a GIS methodology to exclude EEZ areas, globally, that are infeasible for development; namely, protected areas and heritage sites, water

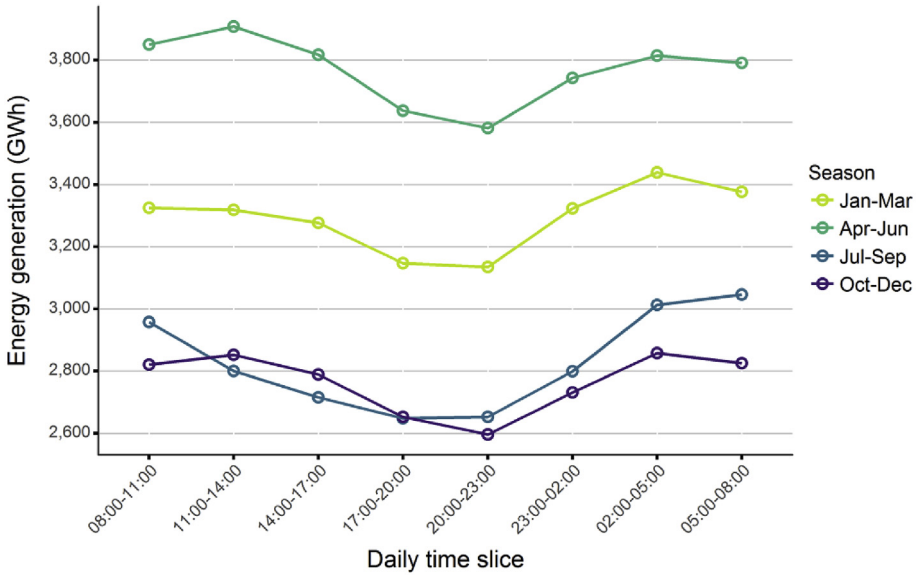

Fig. 12. China's energy generation profile counting the whole capacity potential for 8 aggregated daily time slices over four seasons. April–June has the highest daily generation potential, with almost double the winter (Oct–Dec) output. The diurnal supply profiles are similar across seasons; generation is stronger early morning, with a dip in the afternoon/evening.

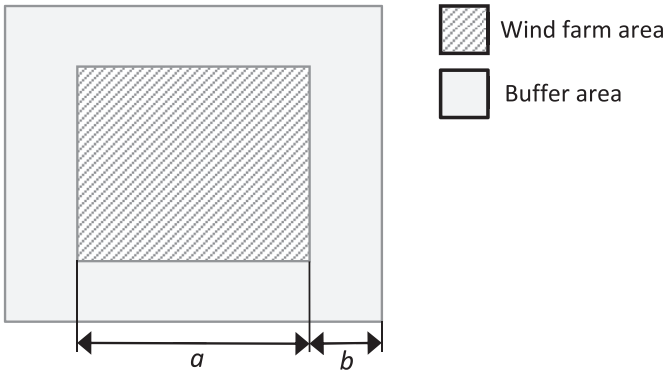

Fig. 13. Representation of a square array wind farm, with area, a^2, surrounded by a buffer zone with area $(a+2b)^2$-a^2, In reality, the whole Exclusive Economic Zone (EEZ) cannot be filled continuously with turbines because of large-array effects which reduce the efficiency of each turbine. In a scenario with significant wind farm deployment, an implicit buffer zone could be imposed, thereby reducing the average capacity density in each EEZ.

depths greater than 1000 m, and a 1 km exclusion zone around submarine cables. The energy generation potential then depends on technology choice, capacity density, and locally-specific capacity factors.

A survey of state-of-the-art turbine technologies led to the inclusion of a 5 MW capacity exemplary turbine with a 126 m rotor diameter and a bespoke nominal power curve, and a hub height chosen at 100 m. Turbine spacing is based on analysis of current wind farm installations and an empirical derivation of array efficiency, leading to a capacity density of 3.14 MW/km^2.

High resolution capacity factors were developed from a unique calibration of two wind speed data sets to retain the high temporal resolution of the MERRA-2 data set and the high spatial accuracy of the Global Wind Atlas. This led to modelled capacity factors that better characterise the wind speed variation close to the coast, and allows the analysis to have a highly granular calculation of generation potential. This treatment improves the reliability and consistency of the data across the globe compared to other studies. Furthermore, two wind speed classes were assumed for this analysis, leading to the development of capacity factors for specific wind conditions, such that the power curve is chosen to better match the wind conditions at each site. The placement of different wind turbines is based on global average wind speeds (from 35 years of NASA MERRA-2 data).

Country-level energy generation potentials (for the entire globe) were calculated using annual average capacity factors from the 32 time slices developed for this work. These outputs could be compared to previous estimates of offshore wind potentials. Table 8 showed that the global energy potential in this study generally overestimates global potentials in comparison. The main reasons were, firstly the increase in spatial scope this study assumed – extending suitable depth to 1000 m - and secondly, the higher resolution and better calibrated wind data, which made possible the grid-wise variation in turbine choice for different wind conditions. It should be noted that the size of wind turbines did not tend to affect the feasible energy density since large turbines have to be placed further apart to mitigate wake interference. Array efficiency was also reassessed for this purpose and at 88.55% for a packing density of 10 rotor diameters, is lower than in many studies.

Table 9 showed that country potentials were sometimes underestimates compared with country-level studies. In those comparisons, the main factor was the reduced spatial feasibility in this study compared to the relative liberal spatial restrictions mentioned in those studies. Another difference was the reduction in energy density used in this study. All the country studies used rather high energy density (5–12.5 MW/km^2) compared to the 3.14 MW/km^2 used in this study, with relatively minor array efficiency corrections, which do not seem feasible from the literature surveyed in this paper. In general, it was shown that country studies over-estimate generation potentials compared to global studies.

This study also showed that reducing the area available in the country EEZ by adding an implicit buffer zone around each wind farm – and reducing the capacity density proportionately – has a big impact on the energy generation available. In the USA, implementing this constraint led to a 70% reduction in generation potential. This effect varies with the size and geometry of the assumed buffer zone, but it is likely that limiting the total area available for

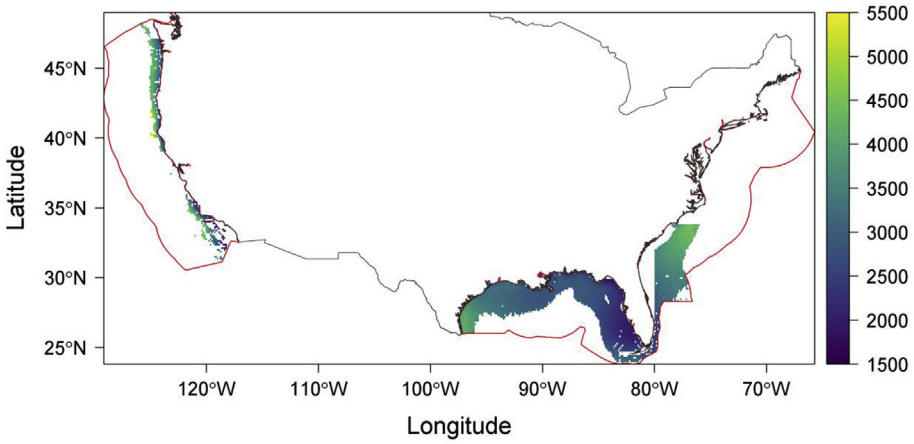

Fig. 14. Energy generation density (MW/km^2/year) in the United States of America offshore EEZ, assuming the energy density is reduced by a factor of 1/3.25 - the ratio of the wind farm array area to the array plus its buffer zone. The Exclusive Economic Zone is outlined in red. Protected areas, the vicinity of subsea cables, and depths over 1000 m are excluded. (For interpretation of the references to colour in this figure legend, the reader is referred to the Web version of this article.)

capacity development with reference to a realistic buffer zone size will improve the capacity potential estimate when considering the whole country EEZ.

This study finds a total offshore wind capacity potential of 85.6 TW (excluding Antarctica) and a total generation potential of 329,600 TWh/year for capacity factors above 20%, and when only suitable areas for development are considered. The average suitable area as a percentage of the Exclusive Economic Zone for each country was 37%. The amount of generation potential is also available in depth classes as well as distance to coast classes. 64,845 TWh is available globally in shallow waters (0–40 m), while 103,852 TWh is located within 10–50 km of the coastline. If only the potentials in locations with the highest quartile (25%) of capacity factors are summed, 83,229 TWh is available.

Future work to improve the reliability of this work will include a multidimensional sensitivity analysis to assess the effects of varying the input variables on the energy potentials estimates. In particular, altering the source and treatment of the underlying wind speeds could help to verify the conclusions of this paper.

Acknowledgements

Jonathan Bosch is supported in this work by The Grantham Institute – Climate Change and the Environment.

Iain Staffell is supported by EPSRC under the funding reference EP/N005996/1.

Adam D. Hawkes is supported by NERC under the funding reference NE/N018656/1.

Appendix B. Supplementary data

Supplementary data related to this article can be found at https://doi.org/10.1016/j.energy.2018.08.153.

Appendix A. GIS input parameters

Table 10 shows a summary of the input parameters of GIS model.

Table 10
Input parameters for the GIS model

Parameter	Value	Additional details
Turbine parameters		
Turbine hub height	100 m	–
Turbine rotor diameter	126 m	RE power 5 M model
Turbine nameplate capacity	5 MW/km^2	RE power 5 M model
Array parameters		
Farm capacity density	3.14 MW/km^2	
Farm turbine spacing	10 RD	
Wake losses factor	88.55%	See supplementary data for empirical derivation, assuming a 10 × 10 wind farm
Turbine availability	97%	
Generation constraint	20% CF	A lower capacity factor cut off for summing energy generation
Geographical parameters		
Water depth constraint	1000 m	Maximum depth for turbine deployment
Water depth categories	0 - 25; 25–60; 60–1000 m	

References

[1] Bruckner T, et al. Climate change 2014: mitigation of climate change. Contribution of working group III to the fifth assessment report of the intergovernmental panel on climate change. In: Intergovernmental panel on climate change; 2014.
[2] Adoption of the paris agreement. UNFCCC; 2015.
[3] The Royal Society. Climate updates: what have we learnt since the IPCC 5th Assessment Report?. 2017 [Online]. Available.
[4] Meinshausen M, et al. Greenhouse-gas emission targets for limiting global warming to 2 °C. Nature 2009;458:1158. 04/30/online.
[5] McGlade C, Ekins P. The geographical distribution of fossil fuels unused when limiting global warming to 2 °C. Nature 2015;517:187. 01/07/online.
[6] IPCC. Climate change 2014: mitigation of climate change. Contribution of working group III to the fifth assessment report of the intergovernmental

panel on climate change (fifth assessment report of the intergovernmental panel on climate change). Cambridge, United Kingdom and New York, USA: Cambridge University Press; 2014.
[7] World Energy Council. Composing energy futures to 2050. 2013.
[8] IEA. Key world energy statistics. 2017. Accessed on: 06/06/2018.
[9] IEA. Energy technology perspectives 2016. 2016 (ETP 2016).
[10] IIASA. Global energy assessment - toward a sustainable future. UK and New York: Cambridge University Press, Cambridge; 2012. NY, USA and the International Institute for Applied Systems Analysis, Laxenburg, Austria.
[11] van Vuuren DP, et al. Alternative pathways to the 1.5 °C target reduce the need for negative emission technologies. Nat Clim Change 2018;8(5):391–7. 2018/05/01.
[12] A. Grubler et al., "A low energy demand scenario for meeting the 1.5 °C target and sustainable development goals without negative emission technologies," Nature Energy, vol. 3, no. 6, pp. 515-527, 2018/06/01 2018.
[13] Loffler K, Hainsch K, Burandt T, Oei P-Y, Kemfert C, von Hirschhausen C. Designing a global energy system based on 100% rwables for 2050: GENeSYS-MOD: an application of the open-source energy modelling system (OSeMOSYS). 2017. DIW Berlin Discussion Paper No. 1678.
[14] Mathiesen BV, Lund H, Karlsson K. 100% Renewable energy systems, climate mitigation and economic growth. Appl Energy 2011;88(2):488–501. 2011/02/01/.
[15] Dupont E, Koppelaar R, Jeanmart H. Global available wind energy with physical and energy return on investment constraints. Appl Energy 2018;209:322–38. 2018/01/01/.
[16] Amanda SA, David WK. Are global wind power resource estimates overstated? Environ Res Lett 2013;8(1), 015021.
[17] Archer CL. Evaluation of global wind power. J Geophys Res 2005;110(D12).
[18] Lu X, McElroy MB, Kiviluoma J. Global potential for wind-generated electricity. Proc Natl Acad Sci U S A 2009;106(27):10933–8. Jul 7.
[19] Miller LM, Kleidon A. Wind speed reductions by large-scale wind turbine deployments lower turbine efficiencies and set low generation limits. Proc Natl Acad Sci Unit States Am 2016;113(48):13570–5. November 29, 2016.
[20] Bosch J, Staffell I, Hawkes AD. Temporally-explicit and spatially-resolved global onshore wind energy potentials. Energy 2017;131:207–17. 2017/07/15/.
[21] European Environment Agency. Europe's onshore and offshore wind energy potential. An assessment of environmental and economic constraints; 2009.
[22] Arent D, Sullivan P, Heimiller D, Lopez A, Eurek K. Improved offshore wind resource assessment in global climate stabilization scenarios. National Renewable Energy Laboratory; 2012.
[23] Turkenburg WC, et al. Chapter 11 - renewable energy. In: Global energy assessment - toward a sustainable FutureCambridge. Cambridge, UK and New York, NY: University Press; 2012. p. 761–900. USA and the International Institute for Applied Systems Analysis, Laxenburg, Austria.
[24] REN21. Renewables 2018 global status report, renewable energy policy network for the 21st century. 2018. Available: http://www.ren21.net/wp-content/uploads/2018/06/17-8652_GSR2018_FullReport_web_-1.pdf (Accessed on: 06/06/2018).
[25] Bloomberg New Energy Finance. New Energy Outlook. 2017.
[26] Krey V, Clarke L. Role of renewable energy in climate mitigation: a synthesis of recent scenarios. Clim Pol 2011;11(4):1131–58.
[27] de Vries E, Milborrow D, Staffell I. Wind turbine trends. ENDS Intelligence; 2017.
[28] Bloomberg New Energy Finance. 1H 2017 offshore wind energy market outlook. 2017.
[29] Offshore Wind Programme Board. Cost reduction monitoring framework. 2016.
[30] Smart G. Offshore wind cost reduction. In: Catapult offshore renewable energy; 2016.
[31] Carbon Trust. Floating offshore wind: market and technology review. 2015. Available: https://www.carbontrust.com/media/670664/floating-offshore-wind-market-technology-review.pdf.
[32] de Boer HS, van Vuuren D. Representation of variable renewable energy sources in TIMER, an aggregated energy system simulation model. Energy Econ 2017;64:600–11. 2017/05/01/.
[33] Pfenninger S, Hawkes A, Keirstead J. Energy systems modeling for twenty-first century energy challenges (in English) Renew Sustain Energy Rev May 2014;33:74–86.
[34] Staffell I, Pfenninger S. The increasing impact of weather on electricity supply and demand. Energy 2018;145:65–78. 2018/02/15/.
[35] Pfenninger S. Dealing with multiple decades of hourly wind and PV time series in energy models: a comparison of methods to reduce time resolution and the planning implications of inter-annual variability. Appl Energy 2017;197:1–13. 2017/07/01/.
[36] Green R, Staffell I, Vasilakos N. Divide and conquer k-means clustering of demand data allows rapid and accurate simulations of the British electricity system. IEEE Trans Eng Manag 2014;61(2):251–60.
[37] Loulou R, Remme U, Kanudia A, Lehtila A, Goldstein G. PART I. In: Documentation for the TIMES model. IEA - Energy Technology Systems Analysis ProgrammeApril; 2005. Available: http://www.etsap.org/tools.htm.
[38] OECD/IEA. Annex J: peri-urban renewable potentials: onshore wind. Energy technology perspectives. 2016. Available: https://www.iea.org/media/etp/etp2016/AnnexJPeriurbanonshorewind_2017_10_05.pdf.
[39] Howells M, et al. OSeMOSYS: the open source energy modeling system: an introduction to its ethos, structure and development. Energy Pol 2011;39(10):5850–70. 2011/10/01/.
[40] Archer CL, Jacobson MZ. Geographical and seasonal variability of the global "practical" wind resources. Appl Geogr 2013;45:119–30. 2013/12/01/.
[41] Hoogwijk M, de Vries B, Turkenburg W. Assessment of the global and regional geographical, technical and economic potential of onshore wind energy. Energy Econ 2004;26(5):889–919.
[42] P. Pfenninger and I. Staffell. Renewables.ninja [Online]. Available: https://www.renewables.ninja/.
[43] Federal ministry of economic affairs and energy (DE). Open Energy Platform [Online]. Available: https://oep.iks.cs.ovgu.de/dataedit/.
[44] NREL. OpenEI [Online]. Available: https://openei.org/wiki/Information.
[45] Cavazzi S, Dutton AG. An Offshore Wind Energy Geographic Information System (OWE-GIS) for assessment of the UK's offshore wind energy potential. Renew Energy 2016;87(Part 1):212–28.
[46] Nagababu G, Simha RR, Naidu NK, Kachhwaha SS, Savsani V. Application of OSCAT satellite data for offshore wind power potential assessment of India. Energy Procedia 2016;90:89–98. 12//.
[47] Hong L, Möller B. Offshore wind energy potential in China: under technical, spatial and economic constraints. Energy 2011;36(7):4482–91. 2011/07/01/.
[48] Pacheco A, Gorbeña E, Sequeira C, Jerez S. An evaluation of offshore wind power production by floatable systems: a case study from SW Portugal. Energy 2017;131:239–50. 2017/07/15/.
[49] Akpınar A. Evaluation of wind energy potentiality at coastal locations along the north eastern coasts of Turkey. Energy 2013;50:395–405. 2013/02/01/.
[50] Musial W, Heimiller D, Beiter P, Scott G, Ram B, Draxl C. Offshore wind energy resource assessment for the United States. 2016NREL2016.
[51] Gelaro RM, McCarty W, Modol A, Suarez M, Takacs L, Todling R. The NASA modern era reanalysis for research and applications, Version-2 (MERRA-2). In: AGU fall meeting abstracts; 2014.
[52] Jake Badger MB, Kelly mark, Larsen Xiaoli Guo. Methodology. 2016, 28/11/. 2016. Available:, http://globalwindatlas.com/methods.html#toc-Section-4.4.
[53] Jake Badger ND, Hahmann Andrea, Olsen Bjarke T, Larsén Xiaoli G, Kelly Mark C, Patrick Volker, Badger Merete, Ahsbahs Tobias T, Mortensen Niels, Jørgensen Hans, Petersen Erik Lundtang, Lange Julia, Fichaux Nicolas. In: The global wind atlas: the new worldwide microscale wind resource assessment data and tools. Technical University of Denmark; 2015.
[54] (2010) V. Intersect of IHO sea areas and exclusive economic zones (version 1). Marineregions.org; 2010.
[55] Flanders Marine Institute. Maritime boundaries geodatabase: maritime boundaries and exclusive economic zones (200NM), version 9. 2016.
[56] IUCN, UNEP-WCMC. The world database on protected areas (WDPA) [Online]. Available: www.protectedplanet.net.
[57] U.S. Geological Survey. Global 30 arc-second elevation (GTOPO30). 2017.
[58] GADM. Global administrative areas 2.8 [Online]. Available: https://gadm.org/data.html.
[59] VLIZ. World marine heritage sites (version 1). 2013.
[60] TeleGeography. TeleGeography submarine cable map. 2018 [Online]. Available: https://www.submarinecablemap.com/.
[61] Staffell I, Pfenninger S. Using bias-corrected reanalysis to simulate current and future wind power output. Energy 2016;114:1224–39.
[62] IEC 61400, 2009.
[63] Loeff Loyens. North sea offshore wind; developments in The Netherlands. 2016. Availablxe: https://www.loyensloeff.com/media/7563/north-sea-offshore-wind-dec2016.pdf.
[64] DECC. Offshore energy strategic environmental assessment. 2009.
[65] Marine Management Organisation. Mapping UK shipping density and routes from AIS. 2014. Available: https://assets.publishing.service.gov.uk/government/uploads/system/uploads/attachment_data/file/317770/1066.pdf (Accessed on: 14/05/2018).
[66] Marine Scotland. AIS - shipping Traffic - average weekly density of vessel types [Online]. Available: http://marine.gov.scot/information/ais-shipping-traffic-average-weekly-density-vessel-types.
[67] European Commission. Maritime traffic density - results of PASTA MARE project. 2010. Available: https://webgate.ec.europa.eu/maritimeforum/en/node/1603.
[68] VLIZ. IHO Sea Areas, version 2 [Online]. Available: http://www.marineregions.org/
[69] Staffell I, Green R. How does wind farm performance decline with age? Renew Energy 2014;66:775–86.
[70] Kruger K. H2 2016 Wind O&M index report. 2016.
[71] IEA. World energy balances 2017. 2017.
[72] Australian Government. Australian energy update 2016. 2016.